
Turbulência

Atila P. Silva Freire
*Programa de Engenharia Mecânica
COPPE/UFRJ*

Anderson Ilha
*Divisão de Metrologia Científica
Inmetro*

Robert Breidenthal
*Department of Aeronautics
University of Washington*

Editores

ABCM – Associação Brasileira de Ciências e Engenharia Mecânica
COPPE/UFRJ – Instituto Alberto Luiz Coimbra de
Pós-Graduação e Pesquisa de Engenharia
IME – Instituto Militar de Engenharia

Coleção Cadernos de Turbulência
Turbulência, Volume 5, Tomo 2.

5^a Escola de Primavera em Transição e Turbulência
Instituto Militar de Engenharia, Rio de Janeiro
25 a 29 de setembro de 2006

Editores

Atila P. Silva Freire, *Programa de Engenharia Mecânica*, COPPE/UFRJ
Anderson Ilha, *Divisão de Metrologia Científica*, Inmetro
Robert Breidenthal, *Department of Aeronautics*, University of Washington

Ficha catalográfica preparada pela Seção de Processos Técnicos da
Biblioteca do Centro de Tecnologia da Universidade Federal do Rio de Janeiro

Escola de Primavera em Transição e Turbulência (5. : 2006: Rio de Janeiro, RJ)
Turbulência: Anais da V Escola de Primavera em Transição e Turbulência,
Rio de Janeiro, 25 a 29 de setembro de 2006 /editores Atila P. Silva Freire,
Anderson Ilha e Robert Breidenthal. Rio de Janeiro: ABCM, 2006.
V, 292 p.; 23 cm – Coleção Cadernos de Turbulência. Turbulência, V. 5)
Inclui bibliografias
1. Turbulência. 2. Mecânica dos fluidos. 3. Fenômenos de transporte.
I. Freire, Atila P. Silva II. II. V EPTT (5. : 2006: Rio de Janeiro, RJ).
III. Associação Brasileira de Ciências e Engenharia Mecânica. IV. Título. II.
Série
629.1332
E74T
ISBN

Copyright 2006, Associação Brasileira de Ciências e Engenharia Mecânica, ABCM.
A ABCM não autoriza a reprodução de qualquer parte desta publicação para sua dis-
tribuição em geral, para promoções, para a criação de novas publicações ou para a venda.
Apenas através de prévia solicitação, por escrito, e em casos.
Documento preparado pelos Editores em L^AT_EX.
Impresso no Brasil pela Gráfica Graffito.

Contents

1	Dynamic response of the near-wall hot-wire/hot-film system and near-wall velocity measurements	1
1.1	Introduction and Contents of Study	1
1.2	Experimental set for determination of the dynamic response (f_D) of hot-wire	4
1.2.1	Rotating disk	4
1.2.2	Marginally elevated hot-wire as a velocity probe	7
1.2.3	Flushed-mounted hot-wire and hot film as wall shear stress probe	8
1.3	The dynamic response of the hot-wire anemometer	9
1.3.1	Near-wall hot-wire for velocity measurement	9
1.3.2	Flushed-mounted hot-wire and hot-film for wall shear stress measurement	20
1.4	The dynamic response (f_D) vis-à-vis electronic perturbation test	31
1.4.1	Square wave perturbation test (f_S)	31
1.4.2	Sine-wave perturbation test (f_{sine})	50
1.5	A model for the frequency response of a near-wall hot-wire	64
1.5.1	A simplified 1-D model for the hot-wire probe	64
1.5.2	Results and discussions on the 1D model	68
1.6	On near-wall hot-wire velocity measurements	75
1.6.1	Calibration of near-wall hot-wire probe for spanwise intensity measurement	77
1.6.2	Mean velocity profile	78
1.6.3	Turbulence flow intensities	81
1.6.4	Turbulence kinetic energy in the viscous sublayer	88
1.6.5	The dissipation rate	90
1.6.6	The convective velocity U_c	96
1.6.7	The integral time scale	101
1.6.8	Concluding remarks for Section 1.6	103
1.7	Overall concluding summary	104
1.8	References	106

2	Cross-correlation digital particle image velocimetry - a review	115
2.1	Introduction	115
2.2	Two-dimensional particle image velocimetry (2D PIV)	117
2.3	General description of 2D PIV	117
2.3.1	2D PIV setup	117
2.3.2	Seeding particles	118
2.3.3	Light sources	119
2.3.4	Light sheet optics	120
2.3.5	Image acquisition CCDs	121
2.4	Fundamentals of cross-correlation particle image velocimetry	122
2.4.1	A visual representation of the cross-correlation concept	122
2.4.2	Statistical description of cross-correlation particle image velocimetry	124
2.4.3	Tracer particle ensemble cross-covariance in physical space	125
2.4.4	Spatial ensemble cross-covariance in projected 2D domain	126
2.4.5	Optimization considerations	128
2.4.6	Digital implementation of cross correlation particle image velocimetry	130
2.4.7	Classical sub-pixel peak finding methods	131
2.4.8	Sources of error	135
2.4.9	Effect of sub-pixel peak finding methods	135
2.4.10	Effect of tracer particle image diameter	138
2.4.11	Effect of tracer particle image shift	141
2.4.12	Effect of tracer particle image density	142
2.4.13	Effect of tracer image quantization levels	143
2.4.14	Effect of background noise	145
2.4.15	Effect of displacement gradients	145
2.4.16	Calculation of differential and integral flow properties from the velocity field	146
2.4.17	Calculation of differential flow properties	146
2.4.18	Calculation of integral flow properties	157
2.4.19	Outlier detection methods	158
2.4.20	Advanced PIV methods	175
2.5	3-D Volumetric measurements	187
2.5.1	Three-dimensional defocusing particle image velocimetry (3DDPIV) method	194
2.5.2	The defocusing principle	195
2.5.3	The descriptive equations	195
2.5.4	Application to flow around a propeller	196
2.6	Concluding remarks	199
2.7	References	199

3	Elements of entrainment	205
3.1	Introduction	205
3.2	Entrainment hypothesis	205
3.3	Entrainment process	206
3.4	Entrainment rate	207
3.5	Acceleration	207
3.5.1	Forced turbulence	208
3.5.2	Temporal self-similarity	208
3.5.3	Exponential jet	208
3.5.4	Super-exponential forcing	209
3.6	Compressibility	210
3.7	Confinement and mixing	211
3.8	Density ratio	212
3.9	Rotation	213
3.10	Stationarity	214
3.11	Stratification	215
3.12	Conclusions	218
3.13	Acknowledgements	218
3.14	References	218
4	New Results on Turbulent Entrainment in Stratified Flows	223
4.1	Introduction	223
4.2	Entrainment theory	224
4.3	Experimental techniques	226
4.4	Turbulent jet impinging on a stratified interface	227
4.4.1	Background	227
4.4.2	Experiment set-up and procedure	227
4.4.3	Results	228
4.4.4	Discussion	231
4.5	Sloping gravity currents impinging on a stratified interface	234
4.5.1	Background on gravity currents	234
4.5.2	Gravity current experiment set-up and procedure	236
4.5.3	Parameters	237
4.5.4	Results	238
4.5.5	Discussion	244
4.6	Thermal/plume impinging on a stratified interface	245
4.6.1	Background on thermals	245
4.6.2	Thermal experiment set-up	246
4.6.3	Results	247
4.7	Conclusions	247
4.8	References	250

Preface

A I Escola de Primavera em Transição e Turbulência (ETT) foi uma iniciativa do Comitê de Ciências Térmicas da Associação Brasileira de Ciências Mecânicas (ABCM). Sonho antigo da comunidade de mecânica dos fluidos, ela se tornou realidade graças ao entusiasmo de alguns pesquisadores e ao apoio generoso de várias instituições.

O grande interesse no assunto, aliado à sua importância tecnológica, foram fatores que sempre conspiraram a favor de sua realização. De fato, por ser a turbulência de interesse geral para vários ramos do conhecimento, o atual formato da conferência sempre foi anseio natural da comunidade. Um fórum onde métodos e práticas pudessem ser discutidos de modo livre se constituía em demanda legítima.

A Escola supriu essa demanda, adicionando, além disso, ao seu escopo, sessões técnicas de alto nível. Fruto principal da Escola, as notas dos mini-cursos dão origem a este livro. Preparadas com enorme dedicação por excelentes pesquisadores e professores em turbulência, elas certamente deverão servir de material didático para um grande número de cursos de pós-graduação em ciências e engenharias afins.

Este volume, portanto, reproduz praticamente na íntegra os textos apresentados na I ETT. No futuro, novas publicações semelhantes a esta serão editadas pela ABCM.

A.P.S.F.

Acknowledgments



Author Listing

Chapter 1

page 1

B. C. Khoo
Dept. of Mechanical Engineering
National University of Singapore
Kent Ridge
Singapore 119260

Y. T. Chew
Singapore-MIT Alliance (SMA)
4 Engineering Drive 3
Singapore 117576

Chapter 2

page 115

Dana Dabiri
Dept. of Aeronautics & Astronautics
University of Washington
Seattle, WA 98195
USA

Chapter 3

page 205

Robert Breidenthal
University of Washington
Seattle, WA 98195-2400
USA

Chapter 4

page 223

Aline Cotel
Dept. of Civil and Environmental Engineering
University of Michigan
Ann Arbor, MI 48109-2125
USA

Chapter 3

Elements of entrainment

3.1 Introduction

Turbulence has been called the most important unsolved problem in all of classical physics. From astrophysics to oceanography, aeronautics to combustion, turbulence is ubiquitous. Yet in spite of its central role in science and engineering, turbulence has defied solution for over a century.

The most important property of turbulence is entrainment. Both transport and mixing in turbulent flows are controlled by entrainment. Boundary layer heat transfer and skin friction are the transport of energy and momentum at a wall. The vertical transport of water and energy in the atmosphere and ocean are determined by stratified entrainment. In high Reynolds number flow, the mixing is entrainment-limited, so much so that the molecular diffusivity can change by three orders of magnitude while the molecular mixing rate changes by only a factor of two. Entrainment determines most of what we really want to know about a turbulent flow.

3.2 Entrainment hypothesis

Half a century ago, Morton, Taylor & Turner (1956) proposed the most successful hypothesis for entrainment. In order to model a thermal rising from the sudden release of buoyant fluid, they argued on dimensional grounds that the local entrainment velocity v_e into the thermal at any station must be proportional to the rise speed W of the thermal at that station. There is simply no other speed available on which to base the entrainment velocity (see figure 3.1). In this way, the thermal grows linearly with height, in accord with observation. Furthermore, their hypothesis is equally valid for a wide variety of other classical flows that might be termed “ordinary turbulence”, correctly accounting for the entrainment rate in the plume, shear layer, jet, wake, etc.

However, the entrainment hypothesis sometimes fails. For example, when the

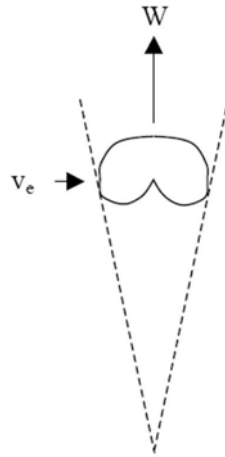


Figure 3.1: Entrainment velocity v_e is proportional to the thermal rise speed W according to the entrainment hypothesis (*Morton et al.*)

speed of sound becomes comparable to the velocity jump across a shear layer, the entrainment rate precipitously declines by a factor of five (Papamoschou & Roshko 1989). This cannot be explained by the original entrainment hypothesis. The entrainment rate is also strongly affected when acceleration, confinement, rotation, or stratification become appreciable. This paper is an attempt to extend the entrainment hypothesis into a more general theory.

3.3 Entrainment process

Entrainment was thought to be a small-scale nibbling process at the edge of a turbulent region. Corrsin & Kistler (1955) proposed a “superlayer” there, across which fluid was thought to be entrained by small-scale nibbling. Shadowgraph images of the supersonic round wake of a projectile seemed to support this notion. However, shadowgraph images of the plane shear layer revealed the engulfment of large tongues of fluid by the largest vortices in the flow (Brown & Roshko 1974; Roshko, 1976). The two-dimensional geometry of their shear layer allowed a more clear view of the entrainment process. Instead of polite little nibbles, their images revealed that the turbulence really entrains like a hungry teenager taking big gulps of fluid. These large engulfed tongues of pure, unmixed fluid are transported by the large-scale vortices entirely across the layer (Konrad, 1976).

3.4 Entrainment rate

The entrainment rate ν_e is a velocity. From dimensional considerations, it must therefore always be expressible as the ratio of a relevant length scale to the rotational period τ_λ of the eddy responsible for entrainment. If there is engulfment, then the relevant length scale must be the size λ of the entraining eddy.

$$\nu_e = \text{const.} \frac{\lambda}{\tau_\lambda} \quad (3.1)$$

Of course, the dimensional argument cannot establish the value of the constant of proportionality. If there is no engulfment, such as at a solid wall or at a strongly stratified interface, the length scale must be a diffusive one, the square root of the product of the diffusivity and an eddy time.

For ordinary, incompressible, free shear flows, the entrainment rate must be proportional to the ratio of the size of the largest eddies to their rotation period. This is a direct consequence of Roshko's engulfment, whereby the first step of engulfment by the largest eddies is rate-limiting. The subsequent processing of the engulfed fluid by all smaller eddies is both proportional to and sufficiently fast compared to the largest eddies that only the largest eddies matter. Since the largest eddies control the rate, we do not need to know much about anything else. This happy circumstance vastly simplifies matters, such as modeling the mixing (Broadwell & Breidenthal, 1982). So for such flows equation (3.1) becomes

$$\nu_e = \text{const.} \frac{\delta}{\tau_\delta} \quad (3.2)$$

where the subscript δ is the size of the largest eddies. Since the characteristic velocity of the turbulent flow is also proportional to δ/τ_δ , we recover the Morton *et al.* entrainment hypothesis for ordinary turbulence. As indicated above, equation (3.2) does not always work. Let us now consider the various violations of the entrainment hypothesis.

3.5 Acceleration

Like people, ordinary vortices slow down as they age. That means that the rotation period of the largest eddies τ_δ increases with time t . In self-similar turbulence, there is no other distinguished time scale, so the period must be proportional to the age of the vortex from its virtual origin.

$$\tau_\delta(t) = \text{const.} t \quad (3.3)$$

For all ordinary turbulence, the constant of proportionality is positive, as is confirmed by examination of the observed growth laws of these flows. Their rotation period always increases with age. These flows are termed "unforced".

Note that the vortex rotation period in an unforced flow may not exactly follow equation (3.3) over a short time interval. For example, the large-scale vortices in

the free shear layer obey equation (3.3) in the long term, but on time scales less than the pairing time, a vortex does not necessarily follow (3.3). We will ignore this subtlety here.

3.5.1 Forced turbulence

However, it is possible to force the flow in such a way that the rotation period does not increase with age. Define an acceleration parameter α such that

$$\tau_\delta = \tau_0 - \alpha t, \quad (3.4)$$

where τ_0 is the large-eddy rotation period at the arbitrary time $t = 0$. For ordinary, unforced turbulence, $\alpha < 0$. If the flow is forced, α can be zero or even positive.

3.5.2 Temporal self-similarity

The vortices are temporarily self-similar if their next rotation period is proportional to their last one. Otherwise there would be a special, distinguished time scale, a contradiction of self-similarity. Figure 3.2 illustrates the evolution of the rotation period of temporally self-similar turbulence. The line must be straight and α must be a constant. For all ordinary, unforced turbulence, $\alpha < 0$ and slopes upward.

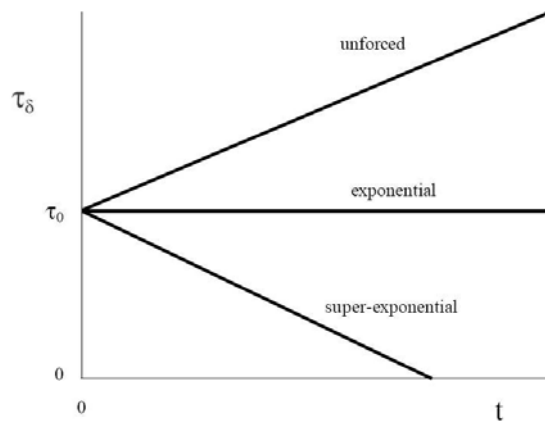


Figure 3.2: Temporal evolution of the vortex rotation period for self-similar flow

3.5.3 Exponential jet

The line is horizontal if the next rotation period is the same as the last ($\alpha = 0$). This can be achieved in an exponential jet, where fluid is ejected from a nozzle with

a speed $V_J(t)$ that increases exponentially in time,

$$V_J(t) = V_{J0} e^{t/\tau_e}, \quad (3.5)$$

where V_{J0} is the nozzle speed at $t = 0$. Because of this forcing, every large-scale vortex in the exponential jet rotates with the same period, equal to the e-folding time τ_e imposed on the flow, no matter how old or how far from the nozzle. The vortices never age. It is a kind of perpetual youth.

Remarkably, acceleration reduces the normalized entrainment rate. A convenient way to measure entrainment at large Reynolds number is with a fast chemical reaction that destroys a visible chemical in the nozzle fluid when mixed with the ambient fluid. If the mixing is entrainment-limited, changes in the visible “flame length” reflect changes in the normalized entrainment rate. Compared to the ordinary jet, the exponential jet has about a 20% greater flame length (Kato *et al.*, 1987). In fact, such acceleration is the only known method for affecting the far-field entrainment rate of the incompressible jet, as noted by Zhang & Johari (1996). Their detailed images of jets with modulated nozzle speed demonstrate that acceleration only influences the entrainment rate when the imposed change in velocity during one vortex rotation is comparable to the initial velocity. In other words, the logarithmic derivative must be appreciable.

3.5.4 Super-exponential forcing

The third category is the line sloping downward in Figure 3.2 ($\alpha > 0$). In spite of getting older, the vortices spin ever faster. After a finite time, the spin rate becomes infinite and the rotation period vanishes.

One might anticipate that the entrainment rate would be further reduced as α increases. Using dimensional and heuristic arguments, one theory has been proposed (Breidenthal (2003) with different notation). The dimensions of the dissipation rate per unit mass are $(length)^2(time)^{-3}$. Every canonical turbulent flow has a conserved quantity Q . For example, in the shear layer, it is the velocity difference ΔU . If the dimensions of Q are in general $(length)^m(time)^{-n}$, the dissipation rate is proportional to $Q^{\frac{2}{m}} \tau_\nu^{-(3-\frac{2n}{m})}$, where the vortex period is τ_ν . For super-exponential forcing,

$$Q = Q_0 e^{\frac{t}{\tau_0 - \alpha t}}, \quad (3.6)$$

where Q_0 is the value of Q at $t = 0$. Define D to be the dissipation rate normalized by that of the unforced flow. From heuristic grounds, we conjecture that the quantity is the natural scaling of effect of α on D . If so, then

$$\beta \equiv - \left(3 - \frac{2n}{m} \right) \frac{dD}{D} = \frac{d\alpha}{-\left(3 - \frac{2n}{m} \right)} \quad (3.7)$$

$$D = e^{-\frac{\alpha - \alpha^*}{\beta}} \quad (3.8)$$

where α^* is the value of α for the unforced flow.

3.6 Compressibility

It has long been known that a compressible flow grows more slowly than an incompressible one. Papamoschou & Roshko (1989) found that the spreading angle of a turbulent shear layer dropped by a factor of about five as the Mach number increased. Linear stability theory may provide an indication of the entrainment behavior, since the underlying instabilities drive the basic flow. However, the indication can only be qualitative, in as much as the finite amplitude eddies are fully nonlinear.

Bogdanoff (1983) recognized that the important parameter for the instability is a “convective” Mach number, the Mach number of the outer flow with respect to the speed of the instability waves. A hint that this is the correct approach comes from the flow models of Brown (1974), Coles (1981) and Dimotakis (1986), discussed below.

One heuristic model that addresses the fully nonlinear flow supposes that nonsteadiness is essential to entrainment. This is a hint of this in the results of the Oster-Wygnanski (1982) experiment, where the vortices in a shear layer are forced to be equally spaced. For a certain time, these vortices are steady, resembling Kelvin’s cat’s eye pattern (Kelvin, 1880), with no vortex pairing. Remarkably, Oster & Wygnanski found that the Reynolds stresses vanish. There is no turbulent transport of momentum. Roberts (1985) found the mixing rate essentially vanishes, in spite of the fact that the vortices are continuing to rotate. If nonsteadiness is required for entrainment, it follows that the signaling speed of acoustic waves must control the physics, since the information about a nonsteady event can travel no faster than the speed of sound.

There is a subtle point to note here. Mach number plays two simultaneous and different roles in high speed flow (Roshko, private communication). On one hand, it indicates the signaling process above. It is also a measure of the energy content of the flow, i.e. thermal vs. kinetic. Indeed, most attempts to model compressibility have focused on energy and density considerations.

The second assumption is that the important time scale for an eddy to entrain is always about one vortex rotation. This is the behavior of the engulfment and mixing process in incompressible turbulence (Brown & Roshko, 1974). The immediate consequence of these two assumptions is that entrainment is controlled by a “sonic eddy” whose rotational Mach number is unity (Breidenthal, 1992). Such an eddy completes one rotation during the signaling time across its diameter. Any larger eddies that might exist would play no role in the entrainment process whatsoever.

The hypersonic wake provides a good opportunity for comparison with experiment. The model predicts that the initial wake growth rate should be zero, since the large-eddy rotational Mach number is greater than unity there. Only sonic eddies, much smaller than the total wake thickness, are capable of transporting momentum. The time scale for the sonic eddies to transport momentum across the entire wake is the square of the wake thickness divided by the product of the speed of sound and the sonic eddy size, this product being the effective turbulent

diffusivity. Note that the concept of turbulent diffusivity is rarely justified.

The initial wake should not grow at all until the rotational Mach number of the largest eddies has fallen to unity. Then the growth rate should transition to the incompressible value. The time for this transition is set by the transport of momentum by the sonic eddies across the width of the wake. Since they are small compared to the width of the wake, the process can be modeled by turbulent diffusion, with a diffusivity equal to the product of the speed of sound and the size of the sonic eddy. Note that for most flows, turbulent diffusion is not an appropriate model (Corrsin, 1974). Only in the rare circumstance of the entraining eddies being small compared with the distance in question is diffusion a reasonable model.

The transition is predicted to occur at a downstream station of M^2d , where d is the effective body diameter. At $M = 20$, this would be 400 effective body diameters downstream, which is in accord with shadowgraph observations (Finson 1973).

3.7 Confinement and mixing

When engineers mix chemicals together, they usually want to retain the mixture in a confined chamber. Examples include combustion and chemical processing. So we will generalize the term entrainment here to include the entire physics of transport and molecular mixing in a confined vessel.

Consider the probability density function (pdf) for the concentration of an inert scalar mixing with a second fluid in some general flow sketched in figure 3.3. Initially the pdf consists of two delta functions at the extrema, corresponding to the two pure fluids. As the turbulence mixes some of the two pure fluids together at intermediate concentrations, forming a central Gaussian in the pdf. For a self-similar free shear layer with two infinite supplies of pure fluid, the pdf would reach a steady state (Konrad, 1976; Broadwell & Breidenthal, 1982). However, if only one fluid supply is infinite, such a finite jet injected into an infinite reservoir, then eventually there is only one delta function in the pdf. If both fluid supplies are finite, then the two delta functions both disappear, and the pdf consists of a central Gaussian, the width of which is the rms concentration fluctuation. As the turbulence further mixes the fluid, the Gaussian progressively narrows and the fluctuations decline.

Here the simplest two assumptions are that both the flow and the mixing are self-similar (Breidenthal *et al.*, 1990). The former requires that the vortex rotation period is proportional to its age, as we have seen above. The latter implies that the concentration fluctuations decline by a factor of e at each rotation. The simple result is that the concentration fluctuations should be proportional to a characteristic time scale τ divided by time.

$$\frac{c'}{\bar{c}} = \text{const.} \frac{\tau}{t} \quad (3.9)$$

The characteristic time scale is determined by dimensional considerations of the problem. For example, if one fluid is initially in a spherical chamber and a second fluid is momentarily injected into the chamber, τ depends on the jet impulse and the chamber diameter. The characteristic time τ must also equal the vortex rotation period at the moment $t = \tau$ when all pure fluid has disappeared and the large-scale vortices have filled the chamber. Measurements of concentration fluctuations are consistent with (3.9), in spite of the fact that the actual vorticity field appears to decay exponentially instead of as inverse time (Aarnio, 1994).

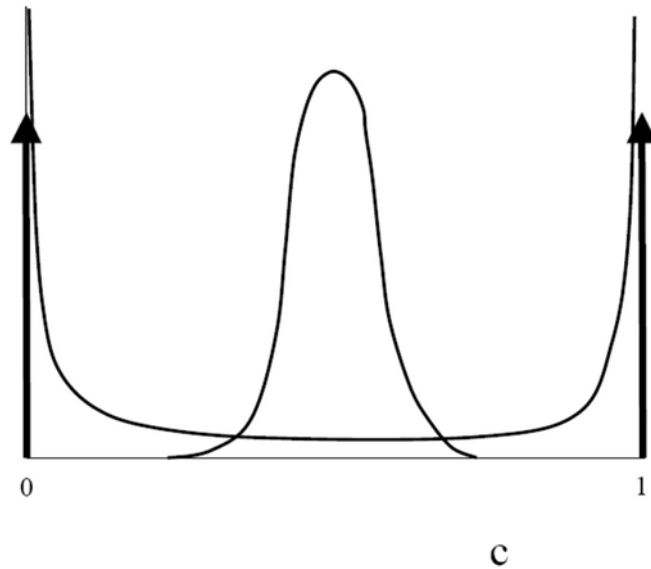


Figure 3.3: Probability density function of the concentration field of a passive scalar is composed of contributions from the pure fluid, Taylor layers, and the vortex cores (Broadwell)

3.8 Density ratio

The coherence of large-scale structure in turbulence was discovered by accident. Brown & Roshko (1974) were attempting to find out about the compressibility effects on entrainment. It was known that supersonic jets exhibited an anomalously low spreading angle. It was not clear if this was due to Mach number or to the density ratio of the supersonic experiments. Since density ratio was easier to control, they elected to measure its effect on spreading angle in incompressible flow by taking shadowgraph pictures. While the most important result of their experiment

was the coherent structure revealed by their pictures, they also determined that density ratio has a remarkably weak effect on entrainment rate. The density ratio must vary by a factor of 49 to achieve a factor of two change in spreading angle. This proved that the main influence on jet spreading angle was Mach number.

A simple picture readily accounts for the effect of density ratio on entrainment into a shear layer. Coles (1981) drew the shear layer in the Lagrangian frame of the vortices (see figure 3.4). Fluid enters a vortex from each stream due to the relative speed of the stream with respect to the vortex. Brown (1974) showed that the relative speed ratio comes from consideration of the stagnation streamlines. Assuming quasi-steady inviscid flow, the total pressure on both streamlines must be constant and equal. Furthermore, the streamlines far from the stagnation point are quasi-parallel, so that their static pressures must be equal. The result is the dynamic pressures of the relative flows far from the stagnation point are equal. So the speed ratio in this frame is just the inverse square root of the density ratio. Dimotakis (1986) neatly summarizes the effects of both density and velocity ratio on both the spreading angle and the entrainment ratio from the two sides of the layer.

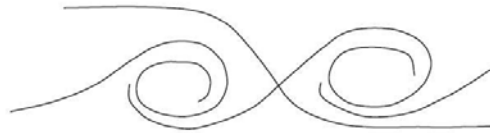


Figure 3.4: Sketch of the flow in the shear layer for an observer moving with the vortices (Brown, Coles and Dimotakis)

3.9 Rotation

Bradshaw (1969) noted that when a fluid rotates, the higher speed fluid tends to want to move to the outside of the turn. This corresponds to a state of lower kinetic energy for the same angular momentum. The difference in kinetic energy between the two states can be dissipated into thermal energy in accord with the second law. On the other hand, if the higher speed fluid is already on the outside of the turn, a rotating flow acts as if it is stratified. This occurs even when the fluid has uniform density. This effective stratification inhibits entrainment.

Cotel (2002) used Bradshaw's analogy to explain the remarkable behavior of aircraft trailing vortices. Even many kilometers behind a large aircraft, the wingtip vortices are compact, laminar cores of only about a meter in diameter, in spite of the large Reynolds number. The radial transport of momentum is strongly inhibited by the effective stratification due to the rotation.

3.10 Stationarity

When a vortex is near a surface, the motion of the vortex with respect to the surface becomes important. The entrainment rate across the surface depends on the amount of stationarity of the vortex. Even a small amount of vortex movement completely changes the physics.

Cotel & Breidenthal (1997,1999) first identified this effect at a stratified interface. The entrainment rate across a stratified interface was much different for an impinging vertical jet compared to other turbulent flows, such as from an oscillating grid. The impinging vertical jet entrained fluid across the interface with stationary, lateral vortices, in contrast to the moving vortices from an oscillating grid or horizontal jet.

In order to quantify the stationarity, Cotel defined a new parameter. The persistence parameter T is essentially the ratio of the rotational to the translational speed of the vortex with respect to the surface (figure 3.5). When T is much less than one, the flow is in the nonpersistent limit. When T is much greater than one, the flow is said to be persistent. For a vortex near a surface, there is no more important parameter than this.

Cotel asserted that the surface may be of any type: a stratified interface, a solid wall, or even an iso-vorticity contour of a neighboring vortex. Thus her theory is applicable to a wide class of flows.

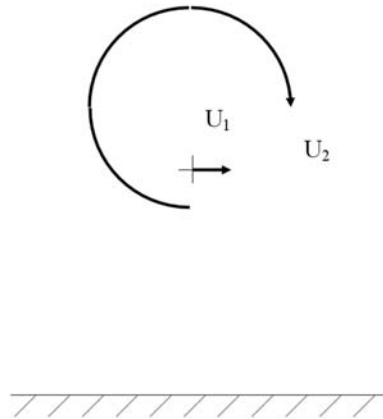


Figure 3.5: The intrinsic velocity ratio of a vortex near a surface - vortex persistence $T = U_2/U_1$ (Cotel)

When a piston suddenly begins to push fluid out of a tube at constant velocity, a starting vortex is formed. The subsequent jet never catches up with this vortex ring (Johari *et al.*, 1997). If the piston advances sufficiently far, the starting vortex cannot accept all the injected vorticity. Gharib *et al.* (1998) defined a

“formation number” to be the ratio of the stroke length to piston diameter. The formation number is essentially identical to the persistence parameter, as noted by Gharib (private communication, 1995). There is a transition in vortex behavior at a critical value of the formation number at about four, when the starting vortex ring can no longer accept all the injected vorticity. This transition is important in heart flow.

Another example of persistence is the boundary layer. When the surface is a solid wall, the wall fluxes can be drastically modified by persistence. In order to achieve the persistent limit, strong stationary vortices must be introduced. This is difficult, since a linear vortex near a flat wall is unstable to both short wavelength Widnall (Widnall *et al.*, 1974) and long wavelength Crow (1970) instabilities, which would promptly render the vortex nonsteady. Balle (Balle & Breidenthal, 2002) suggested that vortices could be stabilized by a wavy wall, substituting for the dividing streamline in a von Karman wake. The wake vortices are known to be at least quasi-stable. Balle found the wall flux measured at the bottom of a trough to be laminar, as predicted by Cotel’s theory. Using flow visualization, Dawson (2005) subsequently confirmed that an otherwise turbulent boundary layer was indeed made laminar by the addition of persistent vortices. However, she found that a small segment of the wavy wall did not achieve laminar flow, due to an adverse pressure gradient in the spanwise direction. It is still an open question if a wall shape can be found that will achieve laminar flow everywhere under persistent vortices. Reducing the heat flux to a laminar value would be useful for turbine blades and hypersonic flow.

Surprisingly, Dawson found that the flow pattern did not correspond to the von Karman wake. Instead, it resembled Kelvin’s cat’s eye flow. As mentioned above, this flow pattern always seems to be associated with laminar fluxes.

These discoveries raise interesting questions about the stabilizing effect of stationary vortices on the flow. It seems reasonable that a stationary vortex would not directly hand off energy into smaller scale eddies, since that presumably requires some kind of nonsteadiness in that vortex. However, the persistent vortex seems to inhibit instabilities even in neighboring vorticity, such as that in the boundary layer below the streamwise vortices. Recent results by Fransson *et al.* (2005) indicate that streamwise vortices can stabilize Tollmein-Schlichting waves.

3.11 Stratification

Based on the persistence parameter, Cotel (Cotel & Breidenthal, 1997) proposed a new model for stratified entrainment. It consists of different entrainment regimes, determined by the Richardson, Reynolds, Schmidt, Prandtl, and persistence parameters. For simplicity, we will only consider the limit of a thin stratified interface.

The Richardson number Ri (of the largest eddies) is defined as the ratio of the potential to the kinetic energy of the largest eddies at the stratified interface. One can also define the *eddy* Richardson number Ri_λ of a smaller eddy of size λ . For

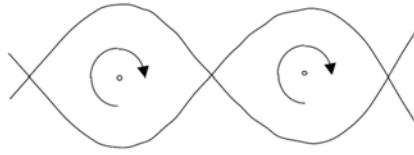


Figure 3.6: Cat's eye flow (Kelvin)

a Kolmogorov spectrum, the eddy Richardson number increases with eddy size.

If $Ri \ll 1$, the potential energy is dominated by the kinetic energy and stratification is not important for any eddy. If $Ri > 1$, there are at least two possibilities. Depending on the Reynolds number, the smallest eddies at the Kolmogorov microscale λ_0 may have an eddy Richardson number Ri_{λ_0} greater than one. If so, then they and therefore all eddies have insufficient kinetic energy to engulf a tongue of fluid across the interface. Consequently, in this limit of strong stratification the interface must be essentially flat. All fluxes are purely diffusive. From dimensional considerations, we can define a corresponding effective entrainment velocity to be the square root of the ratio of the diffusivity divided by some eddy rotation period. The diffusivity corresponds to the flux in question, i.e. mass, momentum, or energy.

There are many choices for the eddy rotation period, ranging from that of the largest to the smallest eddy. Clearly, eddies in the middle cannot be rate limiting, since there is no basis to select one over another. So only the largest or the smallest eddy could be correct. Cotel proposed that in the persistent limit, the correct choice is that of the largest eddy. Remarkably, the fluxes would then be completely independent of any fine-scale turbulence.

While this prediction may not yet have been tested in stratified flow, it does seem to work in the corresponding wall flow discussed above. The heat flux is laminar because the persistent vortices make the flow laminar.

In the non-persistent limit, the fluxes would be controlled by the smallest-scale eddies, corresponding to ordinary turbulent flow. This is in accord with many observations at stratified interfaces and the boundary layer.

If the smallest scale vortices have an eddy Richardson number less than unity, then the interface is not flat. The eddy whose Richardson number is equal to about unity can engulf fluid across the interface. It determines the entrainment rate.

Dramatic evidence of the importance of persistence on stratified entrainment was measured by Cotel *et al.* (1997). Following a suggestion by L. Redekopp (private communication, 1995), they tilted an impinging jet and precessed it. The entrainment rate was reduced by orders of magnitude compared to that of the vertical jet. The effect is not only large, but counter-intuitive.

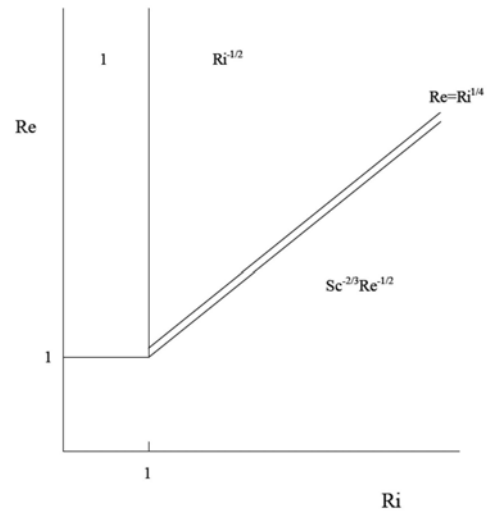


Figure 3.7: Stratified entrainment diagram in the persistent limit (Cotel)

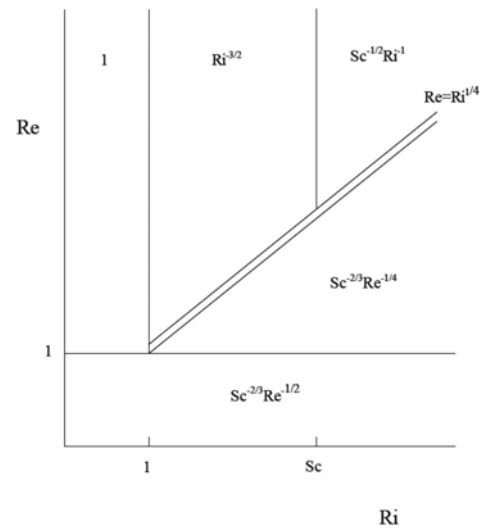


Figure 3.8: Stratified entrainment diagram in the nonpersistent limit (Cotel)

3.12 Conclusions

The entrainment rate of a turbulent flow can always be expressed as the ratio of a length to a time scale corresponding to the entraining eddy. This is a generalization of the entrainment hypothesis of Morton, Taylor & Turner that accounts for a variety of effects, such as acceleration, compressibility, confinement, stratification, and stationarity.

3.13 Acknowledgements

The author would like to acknowledge the contributions of his instructors, colleagues, and students.

3.14 References

- Aarnio M.J.; "Mixing by turbulent streamwise vortices confined in a duct," Ph.D. thesis, University of Washington (1994).
- Balle G. J. and Breidenthal R.E.; "Stationary vortices and persistent turbulence in Karman grooves," *J. Turbulence* **3**, 33-51 (2002).
- Bergantz G. W. and Breidenthal R. E.; "Non-stationary entrainment and tunneling eruptions: A dynamic template for eruption processes and magma mixing," *Geophys. Res. Letters* **28** 3075-3078.
- Bhat G. S. and Narasimha R.; "A volumetrically heated jet: Large-eddy structure and entrainment characteristics," *J. Fluid Mech.* **325** 303-330 (1996).
- Bogdanoff D.; "Compressibility effects in turbulent shear layers, *AIAA J.* **21** 926-927 (1983).
- Bradshaw P.; "The analogy between streamline curvature and buoyancy in turbulent shear flow," *J. Fluid Mech.* **36** 177-191 (1969).
- Breidenthal R. E., Buonadonna V. R. and Weisbach M. F.; "Mixing of jets in confined volumes," *J. Fluid Mech.* **219** 531-544 (1990).
- Breidenthal R. E.; "Sonic eddy - A model for compressible turbulence," *AIAA J.* **30**(1) 101-104 (1992).
- Breidenthal R. E.; "Turbulent stratified entrainment and a new parameter for surface fluxes," in *Recent Research Developments in Geophysical Research*, Pandalai S.G. (editor). Research Signpost, Trivandrum, India, (1999).

- Breidenthal R. E.; "The vortex as a clock," in *Advances in Fluid Mechanics*, Alam M., Govindarajan R., Ramesh O. N., and Sreenivas K. R. (editors). Jawaharlal Nehru Centre for Advanced Scientific Research, Bangalore, India (2003).
- Broadwell J. E. and Breidenthal R. E.; "A simple model of mixing and chemical reaction in a turbulent shear layer," *J. Fluid Mech.* **125** 397-410 (1982).
- Brown G. L.; "The entrainment and large structure in turbulent mixing layers," in *5th Australian Conference on Hydraulics and Fluid Mechanics*, 352-359 (1974).
- Brown G. L. and Roshko A.; "On density effects and large scale structure in turbulent mixing layers," *J. Fluid Mech.* **64** 775-816 (1974).
- Coles D.; "Prospects for useful research on coherent structure in turbulent shear flow," in *Proc. Indian Acad. Sci. (Engng. Sci.)* **4** 111 (1981).
- Corrsin S.; "Limitations of gradient transport models in random walks and in turbulence," *Adv. Geophys.* **18** A, 25 (1974).
- Corrsin S. and Kistler A. L.; "Free-stream boundaries of turbulent flows," *NACA TR 1244*, Washington D.C. (1955).
- Cotel A. J.; "Turbulence inside a Vortex - Take Two," *Phys. Fluids* **14** (8) 2933 (2002).
- Cotel A. J. and Breidenthal R. E.; "Persistence effects in stratified entrainment," *Applied Scientific Research* **57** 349-366 (1997).
- Cotel A. J. and Breidenthal R. E.; "Vortex persistence - A recent model for stratified entrainment and its application to geophysical flows," *Geophysical Flows*, Klewer (1999).
- Cotel A. J., Gjestvang J. A., Ramkhelawan N. N. and Breidenthal R. E.; "Laboratory experiments of a jet impinging on a stratified interface," *Exp. Fluids* **23** 155-160 (1997).
- Crow S. C.; "Stability theory for a pair of trailing vortices," *AIAA J.* **8** 2172-2179 (1970).
- Dimotakis P. E.; "Two-dimensional shear-layer entrainment," *AIAA J.* **21** 1791. "1 shear-layer entrainment", *AIAA J.* **21** 1791 (1986).
- Dimotakis P. E.; "Turbulent mixing," *Annual Reviews of Fluid Mechanics* **37** 329-356 (2005).

Dawson O. R.; "The effect of persistent vortices on boundary layer behavior in flow along a wavy wall," M.S. thesis, University of Washington (2005).

Finson M. L.; "Hypersonic wake aerodynamics at high Reynolds numbers," *AIAA J.* **11**(8), 1137-1145 (1973).

Fransson J. H. M., Brandt L., Talamelli A. and Cossu C.; "Experimental study of the stabilization of Tollmein-Schlicting waves by finite amplitude streaks," *Phys. Fluids* **17**(054110) (2005).

Gharib M., Rambod E. and Shariff K.; "A universal time scale for vortex ring formation," *J. Fluid Mech.*, **360** 121-140 (1998).

Johari H., Zhang Q., Rose M. and Bourque S.; "Impulsively started turbulent jets," *AIAA J.* **35**(4) 657-662 (1997).

Kato S. M., Groenewegen B. C. and Breidenthal R. E.; "On turbulent mixing in nonsteady jets," *AIAA J.*, **25**(1) 165-168 (1987).

Kelvin Lord (Thomson, William T.); "On a disturbing infinity in Lord Rayleigh's solution for waves in a plane vortex stratum," *Nature* **23**, 45-46 (1880).

Konrad J. H.; "An experimental investigation of mixing in two-dimensional turbulent shear flows with applications to diffusion-controlled chemical reactions," Ph.D. thesis, California Institute of Technology (1976); and *Project SQUID Tech. Rep.* CIT-8-PU.

Morton B. R., Taylor G. I. and Turner J. S.; "Turbulent gravitational convection from maintained and instantaneous sources," *Proc. Roy. Soc. A* **234** 1-23 (1956).

Oster D. and Wygnanski I.; "The forced mixing layer between parallel streams," *J. Fluid Mech.* **123** 91-130 (1982).

Papamoschou D. and Roshko A.; "The compressible turbulent shear layer: An experimental study," *J. Fluid Mech.* **197** 453 (1989).

Roberts F. A.; "Effects of a periodic disturbance on structure and mixing in turbulent shear layers and wakes," Ph.D. thesis, California institute of Technology (1985).

Roshko A.; "Structure of turbulent shear flows: A new look," *AIAA J.* **14**(10) 1349-1353 (1976).

Widnall S. E., Blis D. B. and Tsai C-Y; "The instability of short waves on a vortex ring," *J. Fluid Mech.* **66** 35-47 (1974).

Zhang Q. and Johari H.; "Effects of acceleration on turbulent jets," *Phys. Fluids*, **8**(8) 2185-2195 (1996).

